Grant Agreement Number: 801367

Project Acronym: evFOUNDRY

Project title: The Extracellular Vesicle Foundry

Starting Date: 01/09/2018

Project Duration: 42 months

Project Officer: Athina Zampara

Project Coordinator: Paolo Bergese (CSGI)

http://www.evfoundry.eu

D3.5: Integrated modular system for production of EVs

Lead author(s): Ric Gillams, George Attard and Hywel Morgan (SOUTHAMPTON), Bao Dang Ho and Jonas Tegenfeldt (LUND), Lucia Paolini and Paolo Bergese (Brescia).

Contributing partners: SOUTHAMPTON, LUND, CSGI

Due Submission Date: 28/02/2021

Actual Submission Date: 09/03/2021

Status	
Draft	
Final	X

Type		
R	Document, report	
DEM	Demonstrator, pilot, prototype	X
DEC	Websites, patent filling, videos, etc.	
OTHER		

Dissemination Level		
PU	Public	X
CO	Confidential, only for members of the consortium (including the Commission Services)	

Revision History		
Date	*Authors and contributors*	*Comments*
23/02/2021	Ric Gillams (SOUTHAMPTON)	Draft version_v1
24/02/2021	Paolo Bergese, Lucia Paolini, Debora Berti (CSGI)	Draft version_v2
25/02/2021	Bao Dang Ho (ULUND)	Draft version_v3
28/02/2021	Ric Gillams (SOUTHAMPTON), Bao Dang Ho (ULUND)	Draft version_v4
08/03/2021	Ric Gillams, George Attard, Hywel Morgan (SOUTHAMPTON), Bao Dang Ho, Jonas Tegenfeldt (ULUND), Paolo Bergese, Lucia Paolini, Debora Berti (CSGI)	Final version

Essential Glossary	
Acronym	*Meaning*
eDLD	Electrokinetic Deterministic Lateral Displacement
EV	Extracellular Vesicle
PBS	Phosphate buffered saline
PEG	Poly(ethylene glycol)
PDMS	Poly(dimethylsiloxane)
PTFE	Poly(tetrafluoroethylene)

This project has received funding from the European Union's Horizon2020 research and innovation programme under grant agreement No. 801367.

The statements made herein do not necessarily have the consent or agreement of the evFOUNDRY consortium.

TABLE OF CONTENTS

1. NOTICE ON SLOWDOWN AND RESTRICTIONS OF EXPERIMENTAL ACTIVITY BROUGHT BY THE SECOND AND THIRD PANDEMIC WAVES

1.1 PROJECT OVERALL CHALLENGES

Due to the COronaVIrus Disease 19 (COVID-19) pandemic waves (we are being hit by the third one while writing this report), all of Europe has been intermittently on lockdown or under restrictions of some kind since March 2020, with different phased managing strategies employed in different countries, leading to a range of problems and uncertainties. Therefore, most of the evFOUNDRY experiments have been slowed down or interrupted at some level in this period.

This unfortunate possibility was foreseen among the critical implementation risks and mitigation actions (Section 1.3.5. WT5 of the Part A of the Annex 1 of the GA), namely: “Restart after spring 2020 COVID-19 lockdown is slower than expected and/or new COVID-19 lockdown in autumn 2020/winter 2021”. In response, all the partners have constantly taken measures to minimize activity disruption and pursue the objectives and work plan reported in the GA, while ensuring the safety and wellbeing of the researchers and the people with whom they have worked. When necessary, the evFOUNDRY staff has worked remotely, keeping non-experimental activities running and staying connected and prepared for prompt lab activity restart. Indeed, most of the problems the partners have been facing (and still are facing) have been well beyond their control, including lab lockdown imposed by local authorities, sudden quarantine of personnel, shortage and delay in reagents delivery.

The project management board (PMB) examined the partner labs’ experimental productivity during the first 12 months of COVID-19 pandemic in the meeting held on 1st February 2021. The result, summarized in Table 1, outlines a sad overall drop of about 40 % with respect to the pre-pandemic full capacity.

Partner	***Average experimental productivity vs pre-COVID-19 full capacity (March 2020 – February 2021)***
CSGI	50 %
AU	70 %
UU	50 %
ULUND	50 %
SOUTHAMTON	50%
HBM-LS	90 %

Table 1. Average experimental productivity of the evFOUNDRY partners over the latest 12 months with respect to the pre-pandemic full capacity.

1.2 DELIVERABLE D3.5 SPECIFIC CHALLENGES

It must be noticed that evFOUNDRY experimental activity is truly multidisciplinary and interconnected. One single lab lockdown/slowdown may deeply stop/influence activity of the other labs, although the effect has not been uniform across all partner institutions and all WPs.

Some deliverables, such as D3.3, involved work primarily performed by one partner institution. These activities are able to limit the pandemic disruption while others, that rely on close collaboration, have been more directly affected.

In particular, for deliverable D3.5, the work of two partners (Lund and Southampton) needs to be physically connected. The nature of rapid prototyping work in microfluidics is such that there is a large amount of user expertise required for the devices to function well. In deliverable D4.4 we will investigate the feasibility for large scale manufacture. At this stage the devices must be totally robust to be used with minimal training. As such, the devised strategy was that project partners from Southampton would travel to Lund with the prototype devices and the required equipment to run the loading module. This would then be demonstrated in the project partners lab in Lund before investigating the connectivity and integrating the two devices together.

With the travel restrictions enforced to manage the COVID-19 pandemic, it was clearly not feasible for partners to move between labs and, as a result, this strategy had to be discarded. Instead, it was decided that the devices and samples would be shipped by courier as necessary and an online training workshop arranged to enable knowledge transfer from Southampton to Lund.

2. OBJECTIVE OF THE DELIVERABLE

This deliverable finalises the work in WP3 and completes the means of verification for milestone MS3. WP3 objectives were to design and fabricate (i) a loading and (ii) a separation module and (iii) to assemble them in a proof-of-concept integrated system for production of nanosized EVs under flow with steady-state fill volumes of the order of 100 µL. Deliverable D3.3 presents the development work carried out on the loading module. This module uses viscoelastic lift forces to "condition" the sample by removing the largest particles, so that it will be suitable to be processed in the separation module. The development of the separation module is presented in deliverable D3.2. This is based on an electrokinetic deterministic lateral displacement (eDLD) device. The present deliverable (D3.5) is focused on the critical aspect of connecting the modules together in order to realise the benefits of each of the individual modules.

The integration of the modules is a complex process which involves a large amount of planning as well as the correct equipment and approach to ensure that the integrated device works effectively. These different considerations will be presented in the following section. The progress towards the integration is presented in Section 3, 4 and the assembled and tested integrated device is presented in Section 5. Finally, Section 6 reports on the proof-of-concept experiments with bovine milk, provided by partners from Utrecht University (UU).

3. INTEGRATION OF THE MODULES

3.1 OVERVIEW OF INDIVIDUAL MODULES

As described in the original proposal and the arrangement of the WPs, the first stage of the project was to plan the specifications of the individual modules. This provided the key performance indicators for the development of each module individually, with careful consideration of the overall requirements. The design and implementation of the loading and the separation modules have been reported in deliverables D3.3 and D3.2 respectively. Here the key aspects of these designs are highlighted in order to aid discussion of different aspects within this document.

Loading Module

The loading module provides the initial processing of the sample. As a result, it handles the sample while in a relatively heterogeneous state, with a wide range of particle sizes present. In order to handle these samples a simple design is required, avoiding small gaps between features which could easily lead to clogging. To achieve these requirements, a viscoelastic device was conceived, consisting of an inlet (Figure 1(i)), a long narrow channel and an outlet (Figure 1(ii)).

The viscoelastic device uses a polymer additive, for which poly(ethylene glycol) (PEG) was selected, to generate a size dependent lift force on the particles within the channel[1,2]. The design of the channel and the polymer additive were optimised, and this is detailed in deliverable D3.3. In order to take advantage of the size dependent lift forces, the inlet is designed (Figure 1(i)) to produce narrow streams of sample along the top and bottom walls of the main channel. As the sample passes down the channel, the lift forces will move the largest particles away from the walls of the channel. As a result, when the sample reaches the outlet, the smallest particles will remain at the top and bottom of the channel while the largest particles will be in the middle. The outlet produces 3 different streams of liquid, which go to separate reservoirs, as shown in Figure 1(ii, iii).

The designation of these three outlet reservoirs will be referred to as top, middle and bottom. The top and bottom retain the smallest particles, which become the input for the next stage of the sample processing, whilst the middle channel contains the largest particles and as such is a waste stream in the context of EV isolation.

The flow of sample through the device is controlled by two syringe pumps. The sample is pumped into the left-hand inlet reservoir (Figure 1(i)) such that it flows round the loop channel and then flows along the top and bottom walls of the main channel. The right-hand inlet Figure 1(i)) is the sheath inlet. The sheath solution contains none of the sample particles and it simply used to ensure that the sample is in a narrow band close to the top and bottom walls of the channel.

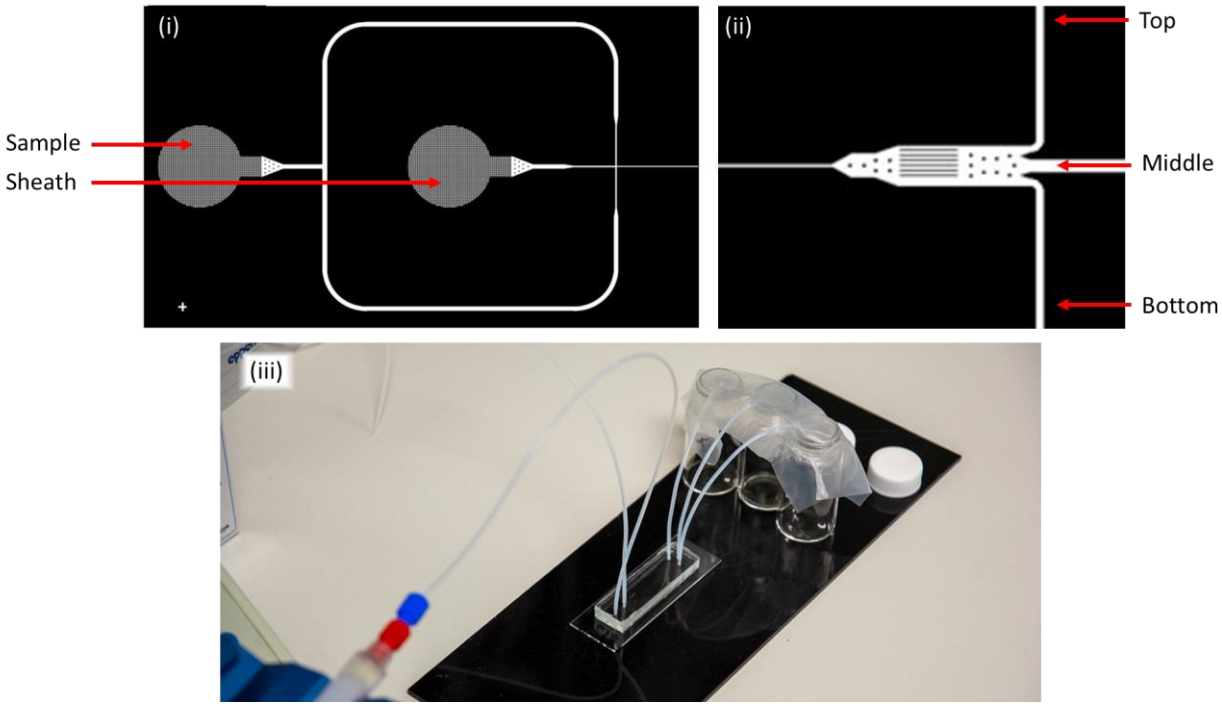

Figure 1. Design of the loading module. (i) The inlet arrangement showing the positions of the sample and sheath solution inlets as well as the loop region which combine the sample into three flows prior to entering the main channel. (ii) The outlet design, including the expansion region, and the three lanes leading to the top, middle (waste) and bottom outlets. (iii) The loading module running with syringe pumps providing the sample and sheath solutions into the inlets and the three outlets being connected to collection reservoirs by Poly(tetrafluoroethylene) (PTFE) tubing.

Separation Module

The separation module performs the fine-tuned separation of the smallest particles in the sample. With the largest particles removed it is possible to use small features in the channel to create a high-precision device. The choice of approach used for the separation module was electrokinetic deterministic lateral displacement (eDLD).

The fundamental principal of deterministic lateral displacement (DLD) is that a tilted array of posts can cause a size dependent displacement of particles in solution. The effect is shown in Figure 2(i). The devices are designed to have a tilted array of posts, meaning that there is a regular distribution

of uniform post in the channel which have a fixed repeat distance. However, moving along the channel, the successive rows of posts are offset slightly, such that the natural path of the posts is not parallel to the direction of the fluid flow. As a result, the fluid flow with zigzag between the posts to maintain a straight net direction. The smallest particles will follow the flow of liquid and zigzag down the channel. This means they will be in a similar lateral position at the start and end of the channel. This behaviour is demonstrated by the green particle in Figure 2(i). If there are particles in the system which are large enough, these will be deflected by the posts in the channel and as such these particles will not be able to conform to the zigzagging path, and instead will bump along the posts and follow the natural incline of the posts. This leads to successive displacement orthogonal to the net fluid flow. This behaviour is demonstrated by the orange particle in Figure 2(i). The determinant for which path the particle takes is the critical diameter of the device. And particle larger than the critical diameter will move in displacement mode, rather than zigzag mode.

In order to utilise this technique for separating nanoparticles, the gaps between the posts can be reduced to generate a critical diameter on the nanometre length scale[3]. However, this approach is very detrimental to volumetric throughput. An alternative strategy is to use an electric field to reduce the critical diameter[4]. This approach has been successfully employed to sort nanoparticles[5,6]. The electric field can be used to reduce the critical diameter of the device. One example of this is taking advantage of the distorted electric field around the posts. This is a result of the posts being electrical insulators (made from poly(dimethylsiloxane) (PDMS)). In this case, the non-uniform field produces dielectrophoretic forces on the particles, which allow smaller particles to follow the displacement path.

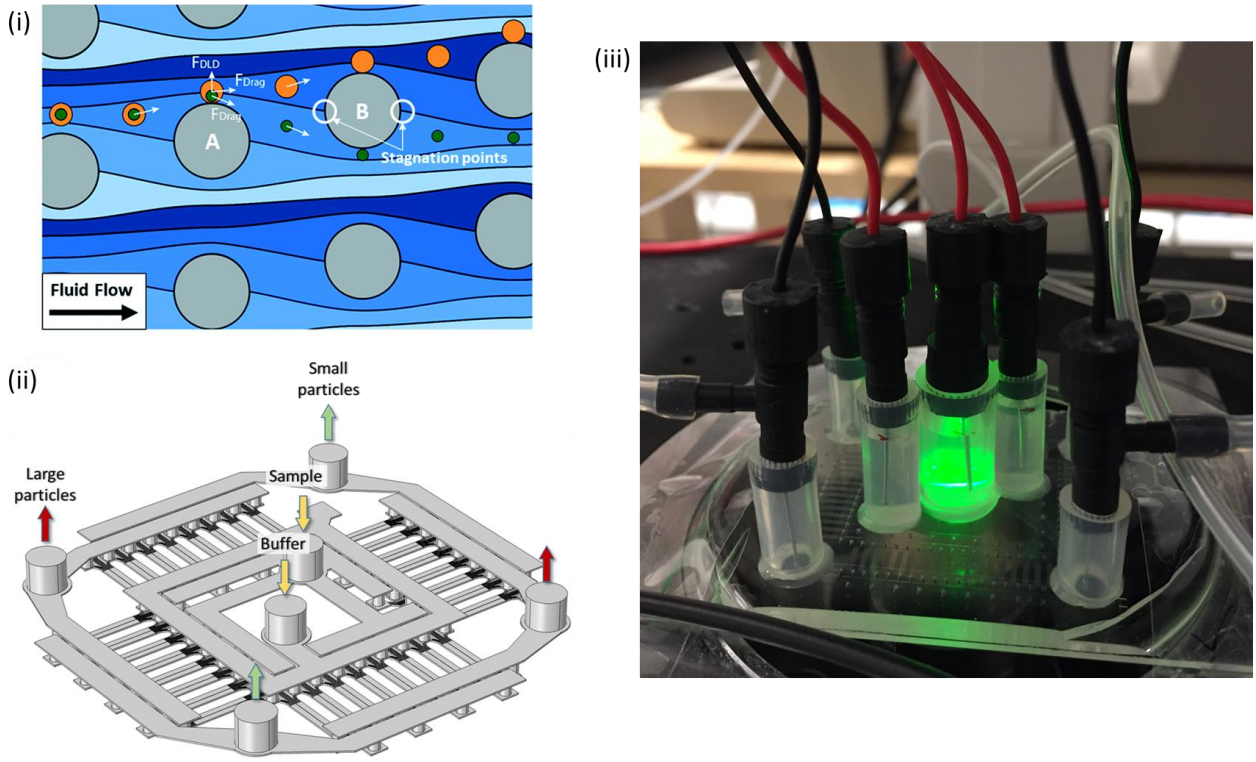

Figure 2. Design of parallel eDLD. (i) Schematic representation of the interaction of particles of different sizes with the posts in a DLD array showing the fluid flow around the posts, highlighting the two pathways for small (green) and large (orange) particles. This is reproduced from recent paper by Calero et al[6]. (ii) The parallel eDLD designed for evFOUNDRY consisting of 64 DLD channels. (iii) The latest generation of the

evFOUNDRY eDLD containing 128 channels, connected to the voltage and pressure supplies and being visualised under a microscope.

The enhanced separation achieved by using electric fields, enables large post separations to be used, which in turn assists with the volumetric throughput of the device. Despite this improvement the throughput of DLD devices is still quite low, tending to be of the order of µL/hr. To meet the specifications for this project, the throughput needs to be significantly enhanced and this can be achieved by running multiple channels in parallel. To simplify the operation of multiple parallel channels, an inlet and outlet manifold was designed, such that the device would be formed of two layers. The top layer handles the fluid distribution, and the bottom layer contains multiple channels which will process the sample simultaneously. A diagram of this design is shown in Figure 2(ii) alongside an operation parallel eDLD device designed for evFOUNDRY (Figure 2(iii)). With this design, the electrodes are inserted into the sample wells and the magnitude and frequency of the electric field can be controlled by the user. An example of the results which can be achieved with this device are shown in Figures 9, 10 and 11.

To control the flow rate of the sample through the device, the sample is loaded into the reservoirs and a positive pressure is applied to those reservoirs, causing a pressure differential across the channels and leading to uniform flow along each of the parallel channels.

3.2 SAMPLE PARAMETER ALIGNMENT

The first deliverable of WP3 was D3.1. This document assessed the requirements of the system as a whole and provided a roadmap for the design and fabrication of the loading and separation modules. By detailing the required input specifications for the separation module, the output specifications of the loading module are defined. The key benefit of deliverable D3.1 was that it created a series of targets and started the discussion, in the consortium, about how these targets should be achieved. During the course of the project these targets have been constantly revisited in project meetings, in order to ensure that any adjustments to the requirements of the separation module can be matched by the loading module. The continuous analysis and discussion of these target variables has been pivotal to the success of this module. The parameters provide the key assessment criteria for each of the modules and have been the targets for device development. These requirements evolved from a combination of knowledge amongst project partners and different constraints applied.

Specification design

The core attribute of the process is the sample. It is essential that the output sample is representative of the input and that the key properties of the EVs are maintained. This means for example that care must be taken not to damage the vesicles or to impair their immunomodulatory function.

The characteristics of the input sample are well understood from discussions with the partners at UU and AU, as well as the visit to both labs in May 2019 (for more details see D5.6, Event participation, Workshops and Training activities list on evFOUNDRY website, RESULTS section, http://www.evfoundry.eu/results/results.php). Furthermore, the final output parameters, to be achieved after the device processing, have being well defined in the first three deliverables of WP1 (D1.1, D1.2, D1.3).

Volumetric throughput

An example of the output driven parameter is the volumetric throughput of the device. In order to biophysically and biologically characterise the output of the devices, it is necessary to combine the expertise of the consortium for each of the different aspects of characterisation. Table 2 shows the list of the essential characterisation approaches, with the relevant partner institution and the volume required for the characterisation. The listed characterisations and related techniques (see D1.1, D1.2, D1.3, D3.3 for more details) require a total volume of ~2 mL of sample. In order to deliver a device for the rapid production of EVs we targeted a time of <6 hours for the production of these samples. This creates the requirement of a throughput of approximately 0.4 mL/hr.

CHARACTERISATION TECHNIQUE	VOLUME	PARTNER
Immunomodulatory properties (T Cell Assay)	Minimum 300 µL. 1 mL for dilution series	UU
Protein markers (Western Blot)	400 µL	UU
Protein number density (Bradford/CONAN Assay)	100 µL	CSGI
Morphology (Atomic Force Microscopy)	100 µL	CSGI
EV number density Nanoparticle Tracking Analysis	100 µL	AU

Table 2. Summary of the off-line characterisation assays to be performed on the output after the device processing.

Conductivity

Other parameters were aligned with the specific requirements of the separation module. The chosen technique for separation by the partners in Lund was the use of the eDLD device. Upon testing and development of this module, it became clear that the voltages required for the effective separation of the size range of interest were high, typically of the order of many hundreds or a thousand volts. Given the conductivity of both milk and *Ascaris suum* media is also high, there are likely to be significant issues with gas evolution and/or heating in the device. This was discussed at length in several project meeting resulting in a decision to lower the conductivity of the sample to achieve a suitable sample for the separation module.

The use of the high voltage in the eDLD device resulted in improved performance regarding throughput. In the early phase of the project, it was believed that the separation of posts within the DLD array would need to be of the order of 1 µm or less in order to achieve an effective critical diameter of the order of 100-200 nm. However, the use of the large field, meant that devices with a post gap of 2 µm were capable of providing the required separation. By doubling the gap between the channel, the resistance of the channel is significantly reduced and so the volumetric throughput is increased. Furthermore, the size requirements for the outlet of the loading module changed as well. If the post gap was to be < 1 µm, then particles close to that size could block the gaps and thus

disrupt the flow of sample through the device, thus rendering it ineffective. With the larger gap size, the requirement for the loading module changed to a 1 µm cut-off.

Flow Controller Hardware

For the integration to be successful, not only do the samples need to be compatible and be produced at the correct rate, but the correct hardware arrangement must be in place to run both devices. Any channel has an associated resistance, which is dependent on the size and shape of the channel, as well as the flow rate and viscosity of the fluid. As such there is a pressure drop across the channel, meaning that the pressure at the inlet and the outlet will be different. This can be overcome in two distinct ways, firstly a pressure differential can be established between the inlet and outlet, usually by applying a positive pressure to the inlet. Alternatively, the liquid can be pushed into the channel at a fixed volumetric flow rate. In this case a syringe pump would be used, and a motor drives the syringe pump at a constant rate, providing whatever force is required to overcome the channel resistance.

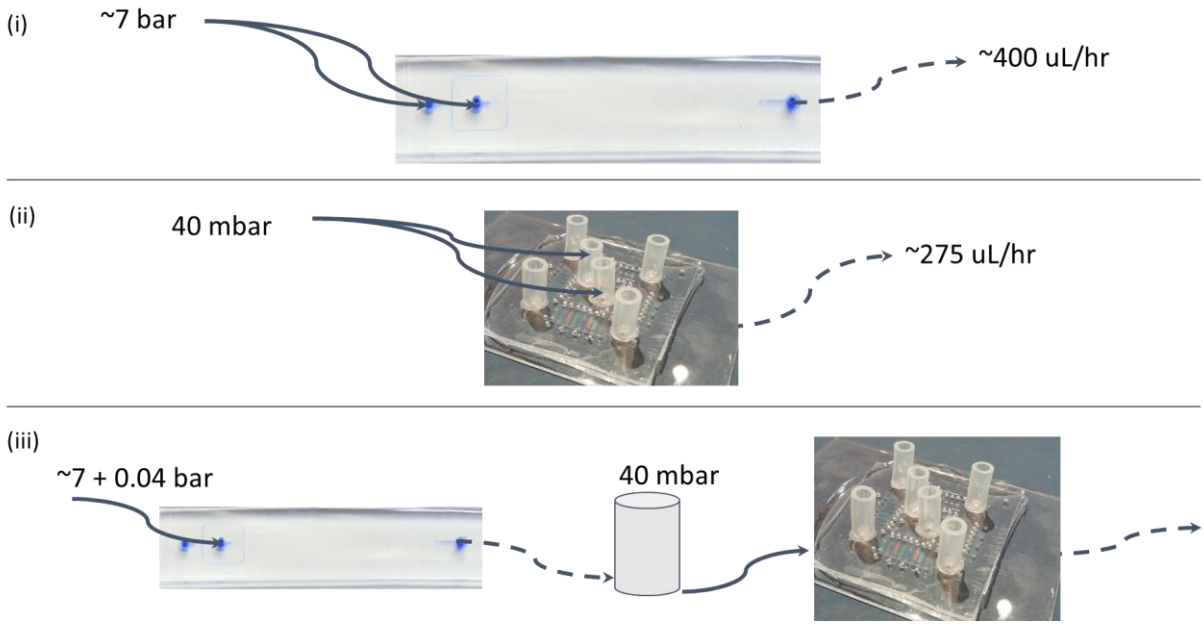

Figure 3. Pressure balanced integration strategy. Running both the loading module (i) and the separation module (ii) by the application of a continuous controlled pressure, would provide the opportunity to have an interconnecting reservoir which would maintain the required pressure differential across each of the modules (iii).

Using one of the two methods it was necessary to generate an approach where the inlet sample could be continuously replenished. For example, it is very hard to introduce additional sample into a syringe *in situ* without introducing air bubbles into the system. Therefore, the syringe could only be used as the initial input into the system and it must be possible for the entire sample to be loaded at once. Similarly, as reported in deliverable D3.3, the trajectory of the particles in the loading module is dependent on the flow rates in the device, so the device must be primed and then the flow rates set. Once the flow rates are fixed, the device should be flushed to achieve a steady equilibrated flow and the flow must stay stable for the duration of the experiment (Figure 3(i)).

The parallel eDLD was designed to use a pressure controller to apply a positive pressure of 40 mbar to the inlets and this pushes the liquid into the channels (Figure 3(ii)). It was shown that the loading

module can be run using pressure controllers as well, although the required pressures are large. This provides a simple route to integration, shown in Figure 3(iii). Essentially the pressure differential required across both devices can be applied to the inlet of the first, so that each device retains the necessary pressure drop to drive the liquid through the device.

Due to the high pressures involved, it was considered more manageable to run the loading module using syringe pumps. It is relatively straightforward to provide pressures less than 1 bar using a benchtop compressor, which makes deployment in partner labs feasible. Testing in Southampton showed that it was possible to run the device into pressurised reservoirs, without impacting the performance of the module. This provided an integration strategy, as the pressurised inlets of the eDLD can then be used as the outlet reservoirs for the loading module. Furthermore, the pressure applied to the outlets of the loading module can be used to fine tune the trajectories of the particles in the loading module.

3.3 PHYSICAL CONNECTIVITY

In order to connect the output of the loading module to the inlet reservoirs of the separation module, a physical connection of the outlet tubing from the loading module into the reservoirs is required. This was achieved in Lund by drilling holes into the side of the inlet reservoirs and sealing the tubing into these holes (see Figure 4). One area of concern was that as the liquid filled the reservoirs, it would reduce the volume of air in the reservoir leading to an increase in pressure, but this was handled well by the pressure controller system, maintaining the consistent pressure required for the correct operation of the separation device. This was demonstrated both in Lund and Southampton, so is a robust solution, suitable for this purpose.

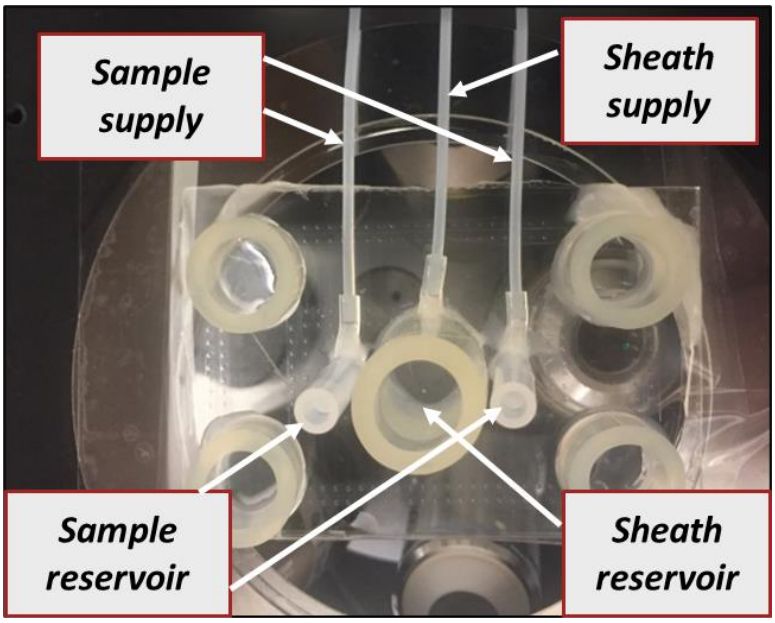

Figure 4. Continuous supply of sample and sheath solution into pressure reservoirs, highlighting the way in which the tubes are joined to the reservoirs.

The only remaining challenge on this front is to ensure that the liquid level is high enough in the reservoir for the electrodes eDLD electrode contact and is maintained throughout the duration of the operation of the device. This should not be a problem given the matched flow rates described in Section 3.2 but depending on the exact pressures and flow rates used, it might be pertinent to run

the loading module for a short time before connecting the pressure controller to the separation device and thus initiating the operation of the separation module.

3.4 REDUCING CONDUCTIVITY

One of the biggest challenges for the integration was handling the conductivity of the samples. Typically, biological systems and buffers contain very high salt concentrations, which are not compatible with the high voltages used in the eDLD. To this end several strategies were explored to bridge the gap between the conductivity of the biological samples and the typical synthetic samples used to develop the eDLD. This difference in conductivity was two orders of magnitude, and so simply diluting the sample with water would have meant a 100-fold decrease in concentration, thus requiring the processing of 100 times more sample in order to collect the same number of EVs. As described in D3.2 and Section 3.1 and 3.2 of this document, the throughput is already challenging and so it was not viable to increase this to such an extent. Ultimately three approaches were taken and when used in combination they provided the required reduction.

Loading module adjustment

The loading module shown in Section 3.1 has two inputs, the sample and the sheath. In order to generate the lift force in the device the polymer additive (600 kDa 0.05% w/w PEG) is required in both the sample and the sheath solution. Initially the sheath solution was designed to be as similar as possible to the sample, the idea was to minimize disruption to liposomes and vesicles, by minimising the osmotic stress. However, in the pursuit of reduced conductivity, the protocol was altered. With the new method the polymer was added to the sample as a solution in deionised water and the sheath solution contained polymer, but no salt. When preparing the sample, the polymer to sample ratio is 1:1 and within the device the ratio of sample:sheath solution is 1:2. This leads to an overall dilution factor of 6. It has been demonstrated that the conductivity of the sample equilibrates between the three inlets along the channel. This has been shown to lower the conductivity significantly.

Separation module testing

Originally the test samples run in the eDLD device were run in 25 mS/m KCl solution. Further testing showed that it was in fact possible to run at higher conductivities, up to approximately 100 mS/m. This was coupled with gaining greater clarity on the separation required in the modules. At 25 mS/m the eDLD was capable of displacing particles even smaller than some of the larger EVs, so by tuning for the required specification, the voltage could be lowered, allowing the device to operate with higher conductivity solutions.

Novel device design

The combination in the improvements from the loading and separation modules, meant that the gap between the conductivity of the biological sample and the module was just under one order of magnitude (as opposed to two orders). Project partners in Lund developed a high-throughput H-filter device. The H-filter takes advantage of the effect of size on diffusion coefficient. The smaller a particle is, the higher the rate of diffusion. As a result, it is possible to design a channel in which the biogenic EVs (typically in the range of 50-150 nm) will not diffuse significantly, whilst the ions will diffuse much more rapidly. As a result, a wide channel can be designed in which a narrow band of sample flows through the middle of the channel (see Figure 5(i, ii)). The inlet and outlet section of the device mirror each other with a thin sample inlet surrounded by low conductivity sheath solution.

As the sample flows down the channel the ions will rapidly diffuse into the low conductivity sheath solution. The EVs will also diffuse, but at a slower rate. By tuning the flow rate, the residence time in the device can be controlled to ensure that there is no significant loss of EVs (Figure 5(iii)) but that there is a significant loss of ions and thus a drop in conductivity. From the bar chart in Figure 5(iv) it can be seen that the inlet sample (left bar) has a high conductivity and the sheath buffer inlet has very low conductivity. At the outlet of the device the two outlets have comparable conductivity with almost a 10-fold decrease in the conductivity of the sample.

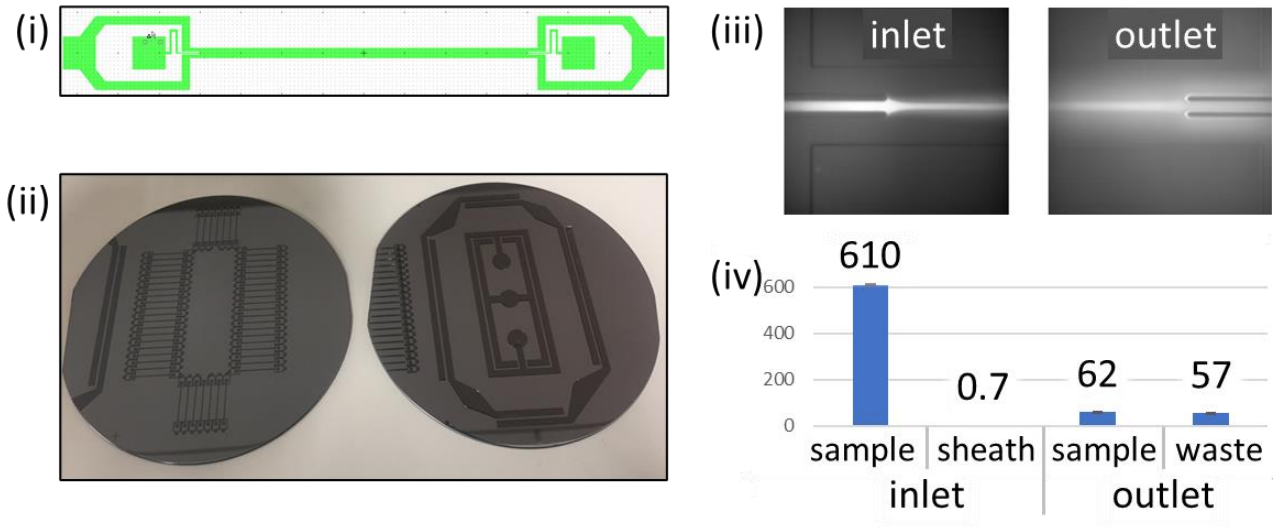

Figure 5. Design of H-filter. (i) A schematic representation of a channel from the device, showing the design of the 3 inlets and mirrored 3 outlets. (ii) Two silicon wafers containing the negative mould of the parallel H-filter design. On the right-hand side, the manifold which handles the samples and feeds them into the 54 identical channels on the left-hand wafer. (iii) Microscope images showing 200 nm fluorescent particles entering and leaving the H-filter device. It can be seen that the vast majority of the particles in the sample exit through the central exit lane, indicating that there has not been significant loss of the particles in the sample. (iv) Bar chart showing the conductivities of the input sample, the low conductivity sheath solution and the sample and waste outlets. This demonstrates that much of the salt in the sample is removed into the waste outlet.

4. PROOF OF CONCEPT

4.1 BUILDING COMPLEXITY

As has been demonstrated with each of the modules in deliverables D3.2 and D3.3, the first testing was carried out using polystyrene beads. This is a critical element of the testing, as the EVs in the biogenic samples do not contain any fluorescent component and so cannot be seen with the microscope. As a result, it is not possible to see the trajectory of the particles and to get instant feedback on the performance of the device. With this in mind, the devised strategy involved sequentially testing the modules in different locations and with polystyrene beads in a low conductivity solution, before shipping the devices, developing the physical connectivity and running the devices in a continuous fashion. Finally, we present data from the biogenic samples showing that the modules can handle the conductivity and complexity of the bovine milk sample

4.2 POLYSTYRENE BEAD SAMPLE MIMIC

The initial proof of concept involved testing the handling of a sample through interconnected modules. With the challenges of travelling to Sweden at this time, a test scenario was developed to test the strategies for connecting modules together. In order to assess the effectiveness of this approach a mimic sample was made up to demonstrate the two levels of separation. The different stages of this experiment are represented in Figure 6. The contained three sizes of polystyrene particle, with diameters of 100 nm, 200 nm and 1 µm. The mixture of polystyrene particles was mixed with 600 kDa PEG in deionised water. Note that for this test of interconnectivity, a low conductivity sample was used for the testing and as such it was not necessary to include the H-filter module described in Section 3.4. This will be revisited in Section 6.1.

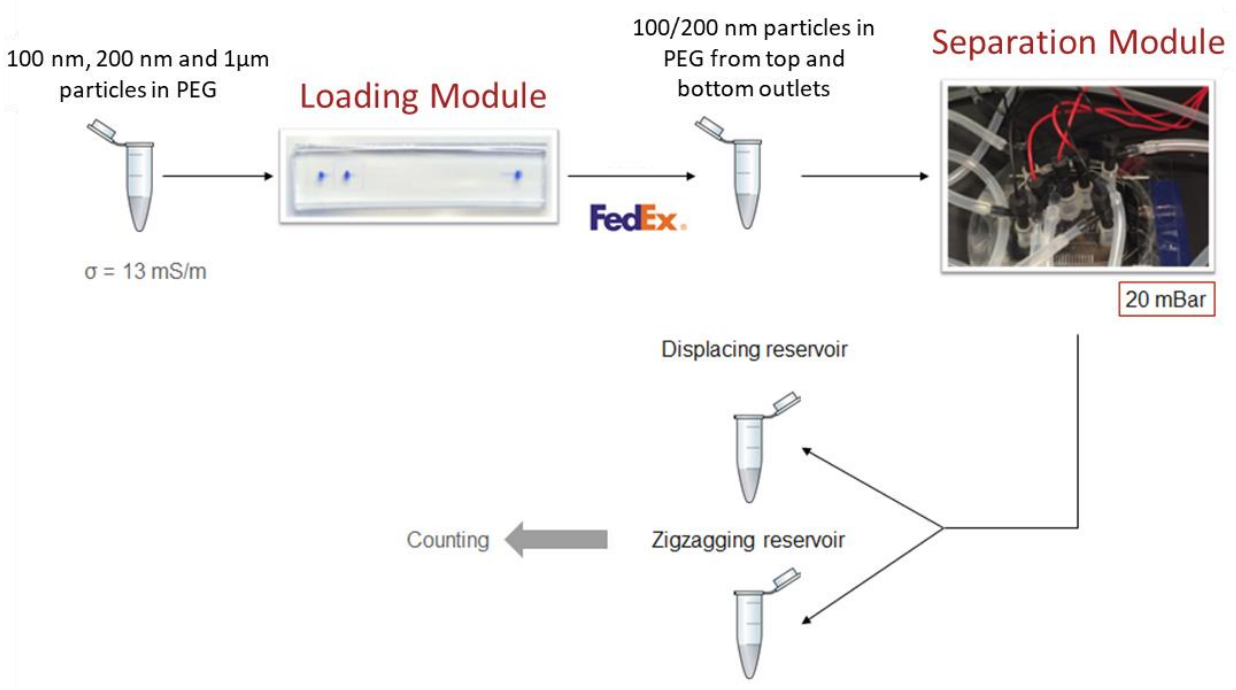

Figure 6. The pipeline for sample handling for the initial proof of concept. A sample was prepared in Southampton of 100 nm, 200 nm and 1 µm particle. The sample was passed through the loading module and shipped to Lund, where it was passed through the separation module. The output of the devices was characterised.

The test sample was prepared in Southampton and passed through the loading module with a sheath solution of PEG in deionised water. The three outlet samples were collected into vials, as shown in Figure 1(iii). The three outlet samples were sent to Lund where the top and bottom samples were run through the separation module. Having passed through the loading module, the 1 µm particles have been removed, into the middle (waste) outlet of the device, whilst the 100 and 200 nm particles remain mixed in the top and bottom outlets of the loading module. The loading module outlet samples were shipped to Lund, where the top and bottom samples were manually transferred into the inlet of the separation module.

When the sample passes through the separation module it will undergo either zigzag around the array of posts leading to a net motion in a straight direction, or it will bump on the posts causing the particles to be successively displaced laterally across the channel. This behaviour is described in Section 3.1 of this document and in more detail in deliverable D3.2. The overall effect is that the original mixture is split in to three separate outlets, containing the 1 µm, 200 nm and 100 nm particles. The polystyrene particles used to produce the initial sample were stained with different fluorescent dyes (100 nm yellow-green and 200 nm yellow-orange). As such it was possible to monitor the particles independently. Figure 7(i) shows a series of microscope images. The top images show the inlet of the device. Both the 100 nm and 200 nm particles enter on the lower half of the device. The upper part is occupied with the sheath fluid which contains no particles. The second row of image show the outlets of the devices when there is no voltage applied. In these images it should be noted that the output section of the devices is designed to contain 8 lanes. The 4 lower lanes continue straight and lead to the zigzag (Z) outlet where particles which have not been displaced will exit the device. The four upper lanes bend away and lead to the displaced reservoir (D). When no voltage is applied to the device, it can be seen that both sizes of particle have flowed straight along the device and so remain concentrated in the lower side of the device. However, when the voltage (1500 V) is applied the larger 200 nm particles move into displacement mode and on the bottom row of images in Figure 7(i) these particles are seen in the upper half and passing into the displaced outlet (D).

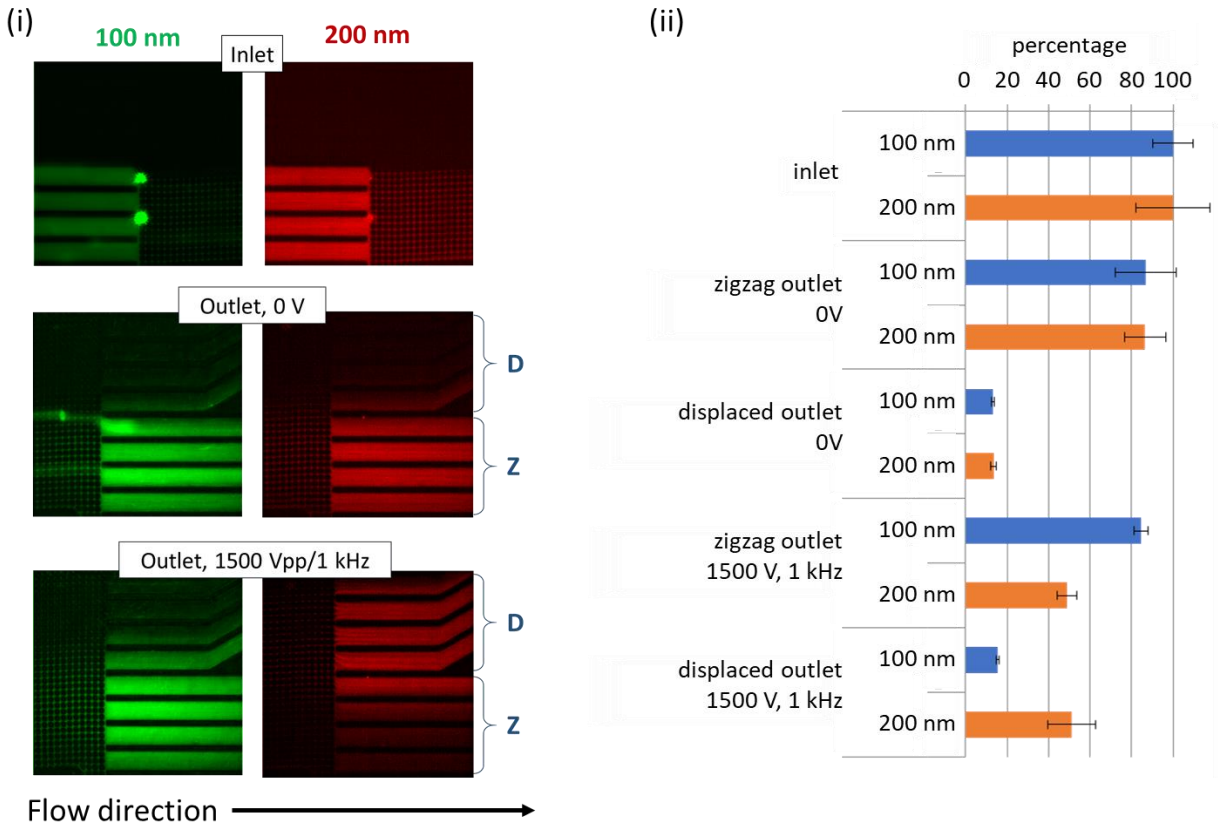

Figure 7. Particle counting data showing the enrichment of 100 nm particles in the zigzag (Z) reservoir. (i) microscopy images captured using two different filter sets, showing in the left-hand column (green) the yellow-green of the 100 nm particles and on the right-hand side (red) the yellow-orange channel of the 200 nm particles. As the voltage is applied the 200 nm particles are deviated to the upper half of the channel and moving towards the displacement (D) reservoir. (ii) Counting data showing the proportion of the particles in each inlet/outlet and the impact of applying a voltage along the channel. There is a marked increase in the presence of 200 nm particles in the displaced outlet when the voltage is applied.

The bar chart in Figure 7(ii) shows the distribution of particle sizes in the separation module. The top bars show the normalised levels of particles in the inlets at 100%. When the device is operated with no voltage applied there is a small amount of lateral diffusion which causes a small subset of each particle size to reach the displaced reservoir, but the majority of the particles of both 100 nm and 200 nm diameter exit through the zigzag outlet. When the voltage is applied, the distribution of particles changes significantly such that the zigzag outlet mainly contains a higher level of 100 nm particles and the displaced outlet preferentially contains 200 nm particles.

5. INTEGRATED MODULAR SYSTEM

The next stage is to run the devices continuously without transferring the sample manually between the two devices. Figure 8 shows the overall assembly of the required equipment and the modules, with further detail provided in Figure 9.

Assembly

The central part of the assembly is the two modules and their connectivity, which will be described in more detail below. Figure 8 shows the overall arrangement for handling the supply of pressure and fluid to the integrated system. The requirements are the supply of sheath and sample solution

to the loading module, the removal of the middle (waste) stream from the loading module, the supply of fresh sheath solution to the separation module and the supply of pressure to the reservoirs of the separation module to drive the solutions down the channel. This is achieved by using three syringe pumps, two connected directly into the loading module and one to preserve the liquid level in the separation module sheath reservoir. The pressure supply is connected to a series of taps, which feed the three inlets of the separation module and the waste outlet of the loading module.

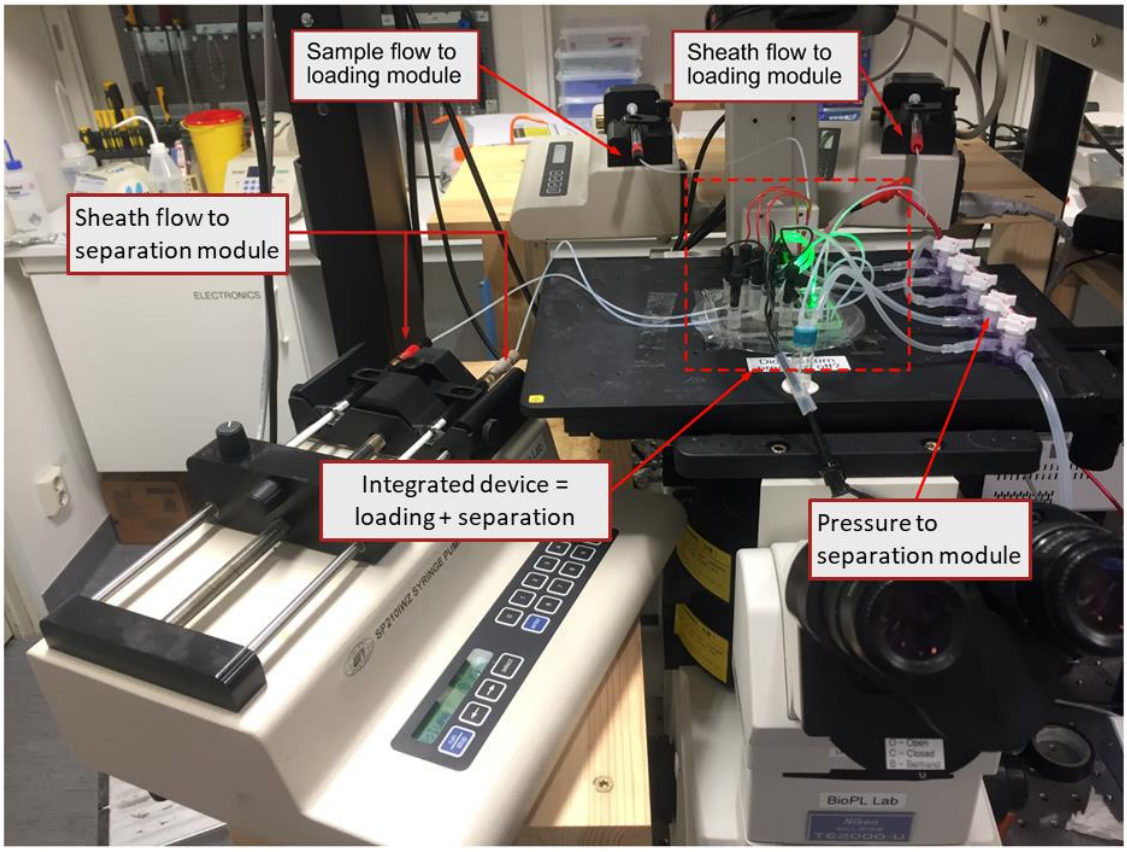

Figure 8. Overview of the complete assembly of the loading and separation modules. The syringe pumps in the background provide the sample and sheath solution to the loading module, which are located on the microscope stage in the centre of the image. The pressure connections are on the right-hand side of the image. An additional syringe pump is used in the foreground to ensure that the liquid level in the separation module reservoir is maintained.

Balancing pressures

As described in Section 3.2, the loading module is operated under a constant flow rate. As a result, the syringe pumps will adjust the force provided based on the resistance of the channel. As discussed above, the result is that if the output of the loading module flows into pressurised reservoirs, then the syringe pumps will generate more force accordingly. As a result, if the three outlets of the loading module are pumped into equally pressurised reservoirs, then the performance of the device should be consistent with the testing done with ambient pressure reservoirs. If however the pressure applied to the reservoirs of the outlets differs then the liquid will preferentially flow to the outlet with the lowest pressure. It is therefore important to balance the pressure of the outlet, in order to be able to remove the middle (waste) stream generated by the loading module. This is achieved by connecting the top and bottom streams to the inlet reservoir of the separation module, which is supplied with 40 mbar of positive pressure, whilst the waster outlet is connected to a vial which is also connected to the pressure supply of 40 mbar. Details of these connections are shown

in Figure 9. One subtle and unexpected pressure effect was caused by the arrangement of the tubing entering the vial for the middle (waste) outlet of the loading module. The vial was kept at a constant pressure of 40 mbar. However, as the liquid reached the end of the tubing, a droplet would form and the surface tension of the liquid would generate a force up causing the flow through that channel to increase, until a drop fell from the tube at which point the forces in the tube would equilibrate. This caused the flow to be unstable and gives an idea of how sensitive the outlets are to the pressure applied.

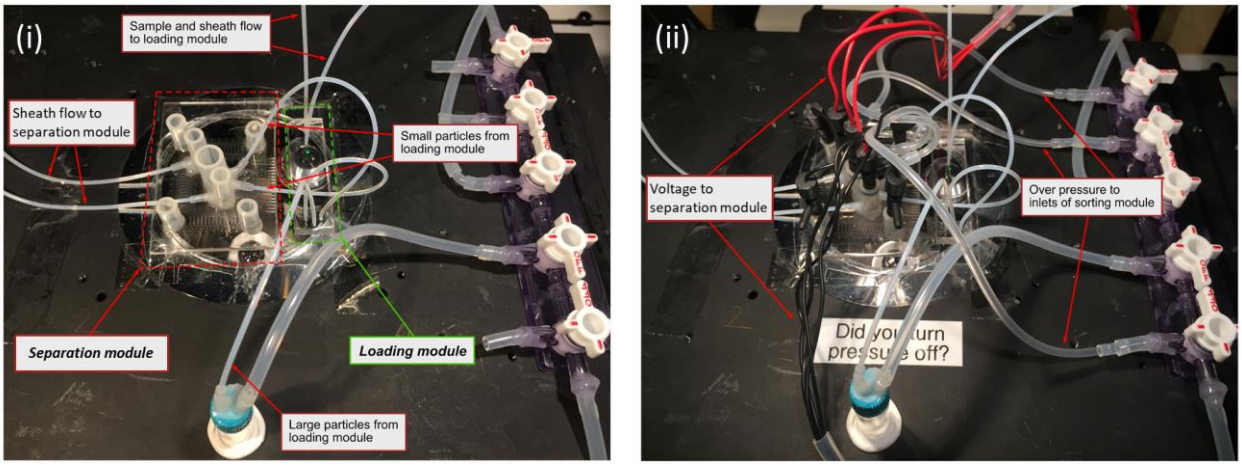

Figure 9. Details of connections for the integration of the loading and separation modules. (i) Fluidic connections and (ii) the complete setup including the electrodes for the separation module. In both images, the pressure supply is shown on the right-hand side and the initial sample inputs come from the top of the picture, provided by the syringe pump.

Visualising the channels

With the two devices aligned side by side on the microscope stage, it is possible to visualise both channels. Again, a synthetic sample was used in the integrated device to enable this direct feedback of the trajectory of the particles, in order to determine whether the device was operating correctly. In this case the particles chosen for this experiment were 1.57 µm, 310 nm and 68 nm. The resulting microscope images allow for the tracking of each component of the system through the two connected devices. On the top row of Figure 10, we track the progress of the 1.57 µm particles. The left-hand image shows the sample entering the main channel. The sample is pinched to the walls of the main channel by the sheath solution and so forms two thin bands at the top and bottom of the channel. The next image is taken at the outlet. By this stage in the channel, the sample is completely focused into a very narrow stream and has been lifted from the walls of the channel into the centre by the viscoelastic lift forces. This image is taken at the exit of the device and so these particles will all leave through the middle (waste) outlet. They will pass down the PTFE tubing and go into the pressurised waste vial.

The second row of images in Figure 10 show the path of the 310 nm particles. Again, they enter the main channel pinched into thin bands at the top and bottom of the channel. As they reach the outlet section of the device, it is clear that they have been lifted away from the top and bottom wall, as there is a dark bank close to the walls, but they are not focussed right into the middle of the channel. As a result, the particles can be seen exiting the device through all three outlets. The brightest bands of intensity are seen leaving the top and bottom exits, which in turn feed into the inlets of the separation module. The blue arrow indicates the connecting tubes joining the loading module outlet to the separation module input and indeed the 310 nm particles can be seen in the bottom half of

the eDLD inlet of the separation module. The top half of the inlet is filled with the sheath fluid. The fourth image in the series shows the outlet of the separation module when no field is applied. In this case the 310 nm particles leave through the lower four lanes, to the zigzag outlet. The final image in this series, shows that when the electric field is applied in the channel, the 310 nm particles move into upper four lanes of the separation module outlet, which feed the displaced particle outlet reservoir.

The final series of images in Figure 10 show the path of the 68 nm particles. These enter the loading module at the top and bottom edge and do not experience significant lift and exit through the top and bottom exits. There appears to be significant diffusion, leading to a wide band of sample and some sample loss through middle channel into the waste outlet. There is a strong signal from the 68 nm particles in the separation module inlet, which predominantly stay in the lower 4 lanes, both in the absence and presence of the electric field.

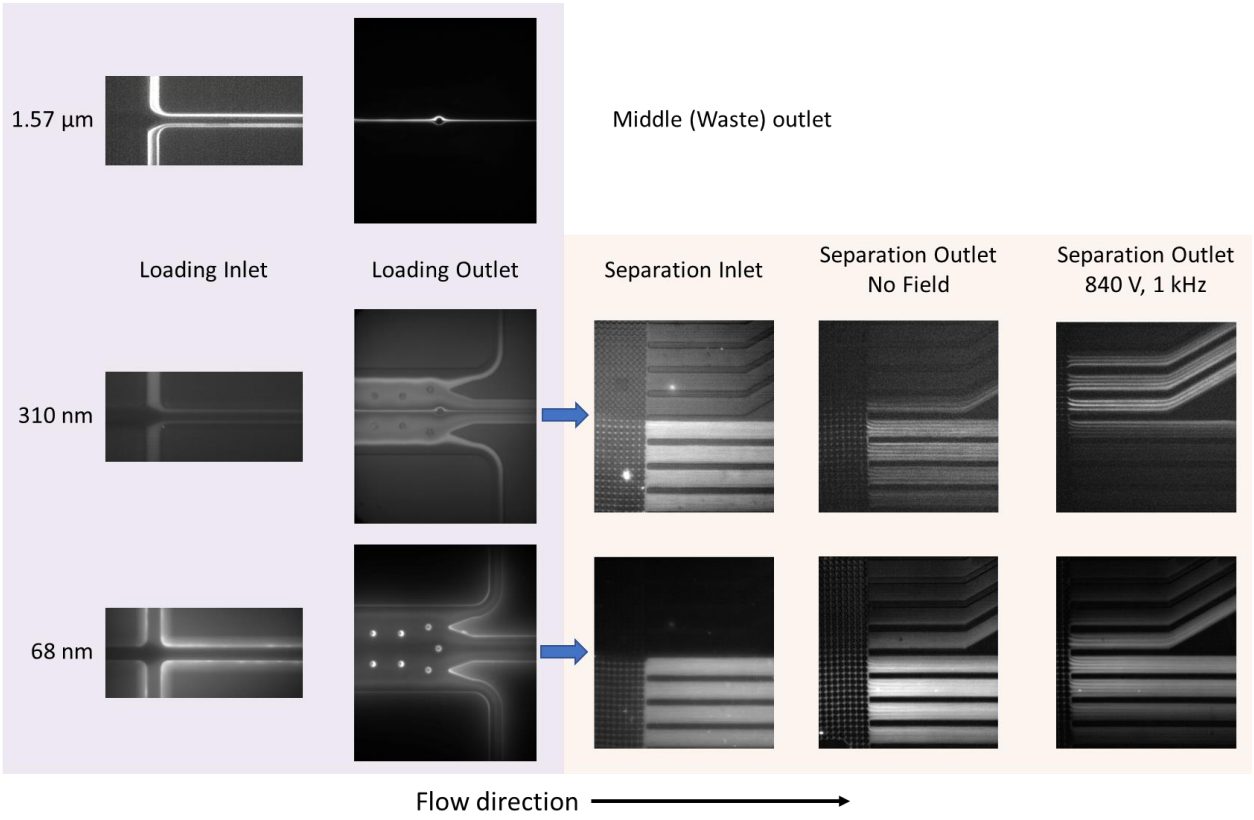

Figure 10. Results from fully integrated device. The full integrated device shown in Figure 8 combine the two modules. In this figure the modules are represented by the coloured backgrounds, purple and orange and the blue arrows indicate the physical connection between the two devices. The three rows of images show the different particle sizes in the input mixture and the five stages from left to right indicate the different parts of the loading and separation modules: Loading inlet, loading outlet, separation inlet, separation outlet (no voltage) and separation outlet (voltage applied). In each case the position of the particles is indicated by the bright areas of fluorescence.

Using the modules in combination, there are three outlets, the loading waste outlet, the separation zigzag outlet and the separation displaced outlet. Figures 8-10 demonstrate that a mixture of three particle sizes can be distributed across these three outlets such that the average size of particles in each outlet is distinct from the other outlets. The largest particles will be found in the waste reservoir and the smaller particles will be preferentially sorted towards the displacement or zigzag reservoir.

6. SAMPLES OF BIOLOGICAL ORIGIN: LAYING THE FOUNDATIONS OF WP4

As highlighted previously, the polystyrene particle solutions make a very convenient test system, but do not include the level of complexity seen in the biological samples. It is therefore necessary to test the system using biogenic samples, given that this will be the use case for the final system.

One aspect of the additional complexity is the conductivity which has been discussed extensively in the earlier sections of this document. As a result of using a sample with higher conductivity it is necessary to leverage all of the tools described in Section 3.4. This includes the use of the H-filter module shown in Figure 5. As such the process becomes a three-step solution, and the proposed integration will follow the same approach described in Section 5 and Figures 8 and 9.

6.1 MILK SAMPLE

The sample used for this test is the one coded M120_2, which is bovine milk treated with EDTA and centrifuged at 10,000 x g (See Table 2 of D3.3 for more details) from UU. This sample was passed through the loading module in Southampton and three aliquots were collected, as is the usual operation described briefly in Section 3.1 (with a complete description presented in deliverable D3.3). The middle outlet is the waste outlet, which will be discarded and then top and bottom outlets contain the samples which are to be processed further in the separation module.

As described in Section 3.4, the loading module setup used PEG (600 kDa, 0.05% w/w) in deionised water to provide the polymer additive. This reduced the conductivity of the sample to approximately 600 mS/m when it left the loading module. The outputs were shipped to Lund and these were passed through the H-filter, resulting in a drop in conductivity to approximately 60 mS/m which is suitable for the separation module.

Polystyrene Spike Experiment

The top and bottom outlets of the loading module are equivalent, due to the symmetry of the device, but for the purposes of this testing they underwent different treatment. In order to provide rapid feedback and trace the movement of particles of different sizes, 100 nm and 200 nm particles were added to the sample, which was then passed through the separation module. The polystyrene beads contained different fluorophores and as such their movement through the separation module could be tracked. Microscope images showing the location of the particles of each size in the inlets and outlets of the separation module are presented in Figure 11. The mixture of 100 nm and 200 nm particles enter the lower four lanes of the inlet. With no voltage applied, both sizes of particle are mainly remaining in the lower four channels at the output and these will be fed into the zigzag outlet. The two images on the right confirm that when a voltage is applied (in this case 150 Vpp at a frequency of 1 kHz) the larger 200 nm particles are displaced and move up towards the top four channels of the exit leading to the displacement module.

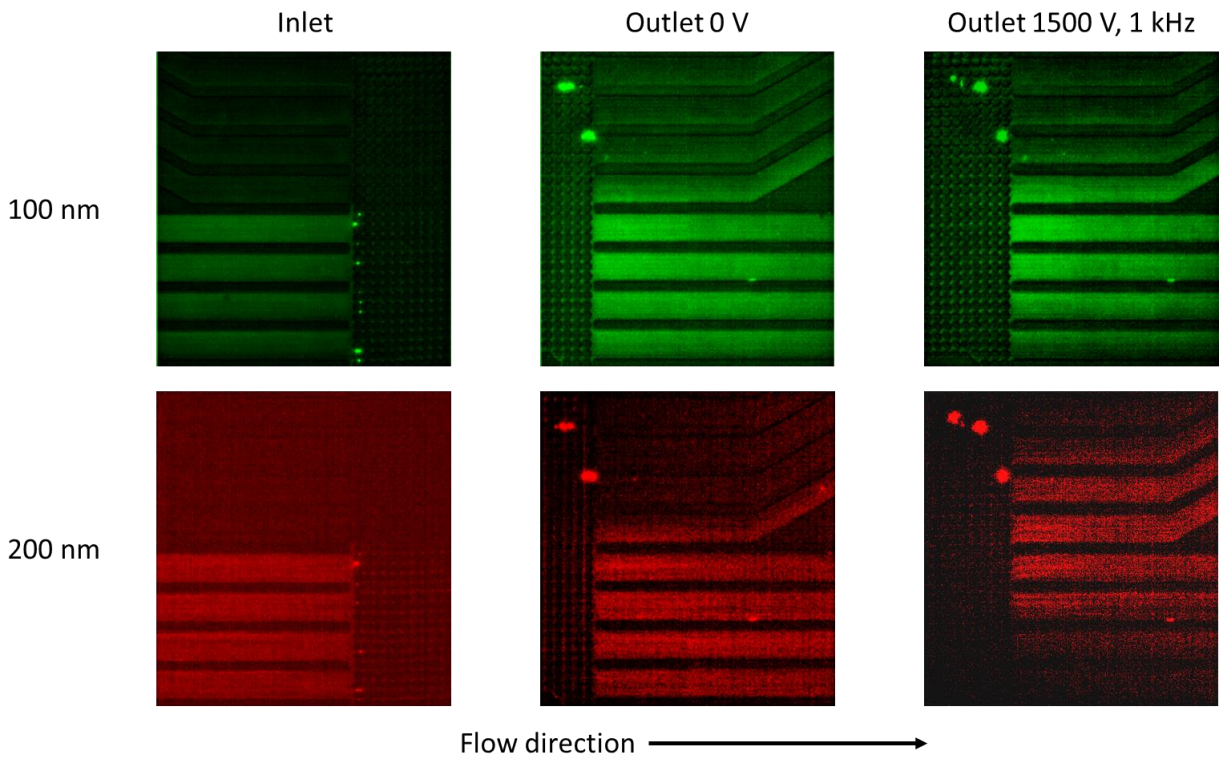

Figure 11. eDLD running milk sample spiked with 100 nm and 200 nm particles. Microscopy images showing the location of 100 nm (top) and 200 nm (bottom) particle at the inlet (left) and outlet (centre, right) of the separation module. The application of a voltage along the channel (right) generates a displacement of the 200 nm particles, causing the particles to move to higher lanes in the outlet of the device.

7. CONCLUSIONS

The work presented in this deliverable is the culmination of the planning and preparation, individual module development and then the integration of these strategies.

The integrated device, presented in Section 5, demonstrated the ability to separate nanoparticles with sizes of 68 nm, 310 nm and 1500 nm. The typical volumetric throughput of the integrated device is of the order of 0.4 mL/hr, in keeping with the requirements which have been identified in the exploratory phase of the project. The volume of the central sample reservoir of the separation module is approximately 125 µL which is in keeping with the targeted steady state fill volume of 100 µL.

The full integration of the modular system, which includes a H-filter for treating the samples of biological origin, requires continued development, but the proof-of-concept devices have clearly shown that these strategies are capable of delivering the fully integrated system. The use of the three modules in Section 6, demonstrates that the key parameters are well understood and can be controlled to enable the full processing of the biological samples to produce nanosized EVs within the device.

8. BIBLIOGRAPHY

1 C. Liu, J. Guo, F. Tian, N. Yang, F. Yan, Y. Ding, J. Wei, G. Hu, G. Nie and J. Sun, *ACS Nano*, 2017, **11**, 6968–6976.

2 D. Yuan, Q. Zhao, S. Yan, S.-Y. Tang, G. Alici, J. Zhang and W. Li, *Lab Chip*, 2018, **18**, 551–567.

3 B. H. Wunsch, J. T. Smith, S. M. Gifford, C. Wang, M. Brink, R. L. Bruce, R. H. Austin, G. Stolovitzky and Y. Astier, *Nat. Nanotechnol.*, 2016, **11**, 936–940.

4 J. P. Beech, P. Jönsson and J. O. Tegenfeldt, *Lab Chip*, 2009, **9**, 2698–2706.

5 B. Ho, J. Beech and J. Tegenfeldt, *Micromachines*, 2020, **11**, 1014.

6 V. Calero, P. Garcia-Sanchez, C. M. Fernandes Honrado, A. Ramos and H. Morgan, *Lab Chip*, , DOI:10.1039/C8LC01416G.